



How to cite this article:

Authors: Tomasz Królikowski, Remigiusz Knitter

Title of article: „Wpływ kąta załamania osi wału, prędkości obrotowej oraz niewyważenia dynamicznego na drgania poprzeczne przegubu homokinetycznego „(“Influence of the angle of collapse of the shaft axle, rotational speed and dynamic imbalance on transverse shifts of the homokinetic joint”)

Mechanik, Vol. 91, No. 3 (2018): pages 256-262

DOI: <https://doi.org/10.17814/mechanik.2018.3.43>

Influence of the angle of collapse of the shaft axle, rotational speed and dynamic imbalance on transverse shifts of the homokinetic joint

Wpływ kąta załamania osi wału, prędkości obrotowej oraz niewyważenia dynamicznego na drgania poprzeczne przegubu homokinetycznego

TOMASZ KRÓLIKOWSKI
REMIGIUSZ KNITTER *

The article discusses analyze issues of drive shafts incorporating constant velocity joints dynamics. It focuses mainly on an impact of a joint on a shaft center support lateral vibrations caused by dynamic loads.

KEYWORDS: drive shafts, CV joint, machine dynamics, unbalance

The articulated shafts are used wherever there is a need to transmit the torque between the devices mounted movably in relation to each other. In practice, the spectrum of use of articulated shafts in industry as well as machines and technical equipment is very wide. The subject of this analysis is the dynamic dynamics of shafts with constant velocity joints of Rzepp. Their basic task is to transfer the torque in automotive propulsion systems (and not only). They are typical for passenger cars with front wheel drive, where it is necessary to transfer the drive simultaneously and steer the direction of travel. In vehicles with a rear axle drive of this type, the shafts replace the Cardan drive shafts when transferring the torque to the main transmission drive axle. They are also commonly used as intermediate shafts in off-road vehicles with wheel drive on both axles.

Turning to constant velocity joints, it should be mentioned that they are used where it is necessary to maintain the same rotational speed of the driving and driven shaft, but for various reasons (e.g. due to lack of space or the need to maintain a low mass) the shaft with two cross joints.

The article focuses on the synchronic joint in its most typical application - as an element of the intermediate shaft of an off-road vehicle.

Purpose of research

The tests are aimed at determining the influence of synchronous joint with length compensation on work dynamics and transverse vibrations of the driving shaft of a motor vehicle, being in the state of unbalance of the dynamic output and receiving shaft.

Construction of drive shafts

In automotive vehicles, the drive shaft is designed to transfer the torque from the gearbox to the drive axle [16]. Due to changes in the vertical position of the components of the drive unit, resulting from deflection of vehicle suspension elements, it is necessary to use articulated shafts. Currently, in automotive technology, drive shafts with three joints (fig. 1) are most commonly used. This is due to the fact that shorter stretches of shafts introduce lower dynamic loads to the drive system than shafts with two joints [19].

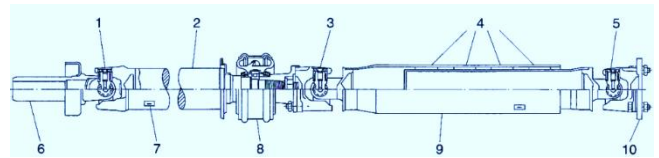


Fig. 1. Typical drive shaft with an intermediate bearing and three gearboxes: 1 - articulated joint, 2 - central shaft, 3 - articulated joint, 4 - vibration isolation, 5 - articulated joint, 6 - sliding element, 7 - load balancing, 8 - intermediate bearing, 9 - shaft, 10 - fork connected to the drive bridge [16]

Constant velocity joints

The traditional joint, the most commonly used in the construction of drive shafts of vehicle vehicles, is the Cardan joint. Its main disadvantage is the unevenness of the rotational speeds of the connected shafts, depending on the angle of refraction of their axes, which introduces unfavorable dynamic phenomena into the system. In the face of increasing requirements regarding acoustic comfort and vibration isolation in vehicles, cross-joints are more and more often replaced with homokinetic hinges. There are many methods to ensure the parallelism of the joint [16], but in the applications related to passenger cars, i.e. the dominant segment of the automotive market, ball joints have become particularly popular. The most important advantage of the constant velocity joints compared to the Cardan joints is to ensure uniform rotational velocity of the receiving shaft, regardless of the angle of refraction of the delivery and receiving shaft axes. This feature is particularly desirable in vehicles with a block drive with front axle drive. Shafts with homokinetic joint are more and more commonly found in the

* Prof. nadzw. dr hab. inż. Tomasz Królikowski (tomasz.krolikowski@tu.koszalin.pl), mgr inż. Remigiusz Knitter (remigiusz.knitter@tu.koszalin.pl) – Wydział Technologii i Edukacji, Katedra Mechatroniki i Mechaniki Stosowanej, Politechnika Koszalińska

construction of classic drives (front engine, rear wheel drive) or all axles [16].

Kinematic analysis

In order to show the difference in the kinematics of the synchronous and asynchronous joints, the differences in the angular velocity of the receiving shaft at a constant speed of the output shaft were simulated. The angle of refraction of the shaft axis is 20° , and the angular speed of the output shaft is assumed to be $360^\circ/\text{s}$. The model of the Velcro joint was used as a model for simulation (fig. 2). The results (fig. 3) confirmed significant fluctuations in the speed of the driven shaft via the gimbal joint and the uniform speed of the shaft driven by the synchronous joint.

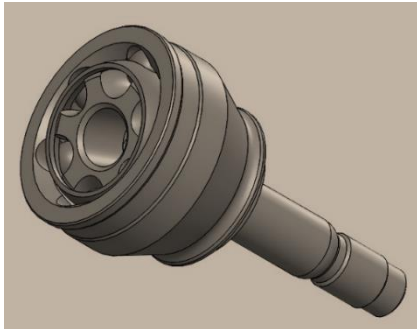


Fig. 2. Joint model used in the simulation (own study)

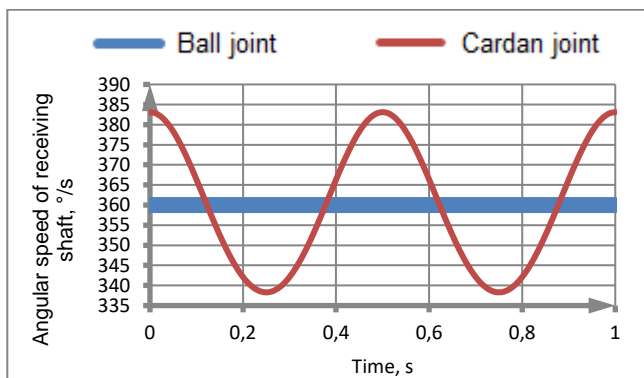


Fig. 3. Comparison of the speed of receiving shafts driven by the Rzepp and Cardan versions (own study)

This is consistent with the information available in the scientific literature. The synchronous joint transmits the rotational speed of the driving shaft - without changing the value and without distortion - to the driven shaft, whereas in the case of the gimbal, uneven angular velocity of the driving and driven shaft can reach 13% or more depending on the angle of the axis between the shafts [8].

Equilibrium conditions of the constant velocity joint

The following conditions must be met in order for the joint to work properly:

- all momentum transfer balls must be located in one plane, the so-called the homo-kinetic plane;
- homokinetic plane must be self-aligning so that it always divides the angle of fracture of the shafts into half;
- symmetry axes of the component shafts should intersect at one point on the plane.

It is obvious that in order to ensure trouble-free operation of machines, they should operate at frequencies far from the frequency of their own vibrations [20]. This also applies to the research described in the article.

Using the relationship between the circular frequency and the vibration frequency, for a given resonant frequency f_0 (in Hz) the proprietor's own vibration can be determined by the

resonant circular frequency of oscillations ω_0 (in rad/s), i.e. the rotational speed at which resonance can occur:

$$\omega_0 = 2\pi f_0 \quad (1)$$

$$\omega_0 = \frac{\pi n}{30} \quad (2)$$

where: n - rotational speed (in revolutions), at which, due to unbalance, a resonance of the center support occurs.

After transforming dependencies (1) and (2):

$$n = 60f_0 \quad (3)$$

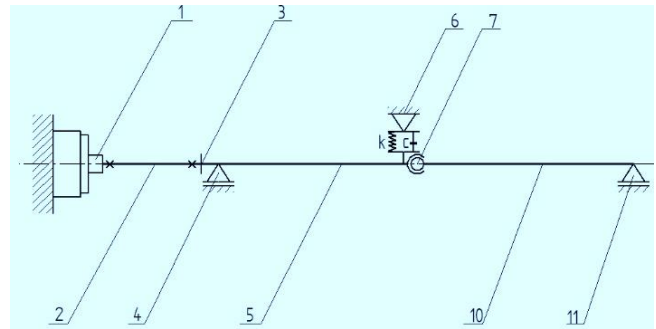


Fig. 4. Kinematic scheme of the measurement stand: 1 - main shaft of the balancing machine, 2 - intermediate shaft, 3 - flange connecting shafts, 4 - initial support, 5 - drive shaft, 6 - central support, 7 - joint, 10 - driven shaft, 11 - end support, k - coefficient of elasticity of the central support, c - damping coefficient of the central support (own work)

The natural frequency of the tested central support is approximately $f_0 = 2$ Hz [6]. After substituting this value for the equation (3), $n = 120$ rpm was obtained. Considering the fact that the lowest rotational speed of the shaft used in the tests is $n = 800$ rpm, it can be considered that this value is sufficiently distant from the resonant frequency of the support and that the pre-existing condition is met.

Characteristics of the measuring apparatus

The main sensor used to record the results of measurements was the Bently Nevada vibration transducer from the 9200 series. It was mounted on a central support using a magnetic base. This sensor directly registers the value of the amplitude of the vibration velocity, however, it is also possible to electronically integrate or differentiate the signal in order to obtain the amplitude value of displacements or accelerations of the vibrations of the support. Series 9200 sensors are made of a coil of copper wire, wound double in opposite directions (in order to eliminate the inductance of both windings). The coil moving in the magnetic field generates a measurement signal recorded by the analyzer [2]. The sensor used is adapted to work in the frequency range $10 \div 1000$ Hz, while the maximum recorded displacement is 2.54 mm [2]. The characteristics of the sensor fully correspond to the intended applications. The rotational speed of the shaft is measured contactless using a photo sensor, which counts the pulses generated by reflection of the light beam from the reflective element mounted on the examined shaft. The collected pulses are processed into the speed value in the Bently Nevada TK84 measuring interface [4]. Data collected directly from the vibration speed converter and processed by the TK84 interface are supplied - for further processing and presentation - to the Bently Nevada TK83 vibration analyzer. This recorder allows for integration and differentiation of the signal, and in addition - for direct reading of the amplitude of the measured quantity and its phase angle [3].

Preparation of the joint for testing

To enable the imbalance to be entered, two discs have been made with threaded holes around the circumference. They were installed on the shaft (in its driving and driven part), maintaining the perpendicularity of the face of each disc to the axis of rotation of the shaft. Thanks to this treatment, axial run out was eliminated. Because the diameter of the tested shaft was much larger than the maximum possible to be placed in the end support, it was necessary to make an appropriate reduction plug. This element was rolled and welded at the end of the shaft. The shaft was subjected to dynamic balancing and then mounted on a test bench (fig. 5).



Fig. 5. Shaft placed on the test bench (own study)

According to ISO 1940-1: 2003, balancing is a procedure based on adjusting the rotor mass distribution in a way that ensures that the residual unbalance remains within limits dependent on the rotor type, its mass and the maximum working rotational speed [10]. The unbalance condition exists in the case when the main central rotor inertia axis does not coincide with its axis of rotation. In the case of rigid rotors, it is possible to reduce the system of forces and present the state of non-balancing using the vector and the moment of the main non-balancing (fig. 6). Starting from the equilibrium of forces and moments, one can decompose the vector N_s into two parallel vectors operating in any planes N_{Is} and N_{IIs} . Similarly, the vector of the moment of the main imbalance of M_N can be divided into the constituent vector N_{Im} and N_{IIm} of forces, the sum of which is equal to the moment M_N . By assembling the N_{Is} and N_{Im} force vectors and (analogously) N_{IIs} and N_{IIm} , a vector representation of the acting unbalance is obtained, described with the N_I and N_{II} force vectors [16].

On the basis of the rotor type, the accuracy class of its balancing should be determined using the tables available in the said standard. Then determine the mass of the shaft (in kg) and its maximum working speed.

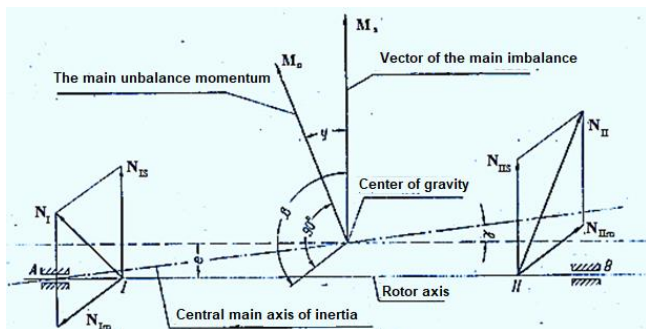


Fig. 6. Representation of the main vector and unbalance moment [16]

The maximum permissible unbalance U_{per} ($g \cdot mm$) can be determined from the dependence:

$$U_{per} = 1000 \cdot \frac{(e_{per} \cdot \Omega) \cdot m}{\Omega} \quad (4)$$

where: e_{per} - unit residual unbalance, $g \cdot mm/kg$; $(e_{per} \cdot \Omega)$ - coefficient associated with balancing accuracy class, mm/s ; m - element mass, kg ; Ω - working angular speed, rad/s .

TABLE I. Accuracy classes balancing rigid rotors [11]

Machine type	Quality class G	Coefficient $e_{per} \cdot \Omega$, mm/s
Car wheels, wheel rims, drive shafts	G 40	40

According to the standard, the tested shaft should be balanced in class G 40 because it comes from a passenger car. Dynamic three-plane balance is the last stage of preparing the test shaft.

Assumptions and scope of research assumed

To limit the number of variables and to facilitate the analysis of results, the assumptions were made:

- one homo-kinetic joint has been isolated from the tested shaft,
- angle of refraction of the shaft axis changes in a range of $0 \div 15^\circ$ in increments of 5° ,
- rotational speed of the shaft is in the range of $800 \div 3000$ rpm,
- unbalance applied is a maximum of $2600 g \cdot mm$ (40 g mass load applied on a 65 mm radius) and the phase angle of the unbalanced vector inserted ranges from $0 \div 351^\circ$.

To achieve the assumed research goal, they were planned as follows:

- reference measurement - measurement of the amplitude of the transverse vibration velocity of the shaft and its phase angle as a function of the shaft rotational speed (at zero angle of refraction of the axis and residual unbalance),
- determining the dependence of the functional amplitude of the transverse vibration velocity of the shaft and its phase angle on the angle of refraction of the shaft of the output and receiving shaft and the speed of rotation of the output shaft,
- assessment of the impact of the introduced unbalance in the part of the driven shaft at constant rotational speed and variable angle of refraction of the shaft of the delivery and receiving shaft,
- assessment of the influence of the phase angle of the unloaded input of constant value in the output and output part of the shaft at the constant angle of refraction of the delivery and receiving shaft axes.

Method of testing

In the experiment, it was decided to measure the value of vibration velocity amplitude as a quantity that well reflects the vibroacoustic state of the machine, because it is proportional to the energy flows passing through the machine node evaluated [7, 12]. In addition, this value is measured directly by the measuring transducer and displayed on the analyzer screen. The next measured parameter was the phase angle of the amplitude of vibration velocity at the center of the center support (fig. 7). This value can also be read directly from the measuring apparatus.

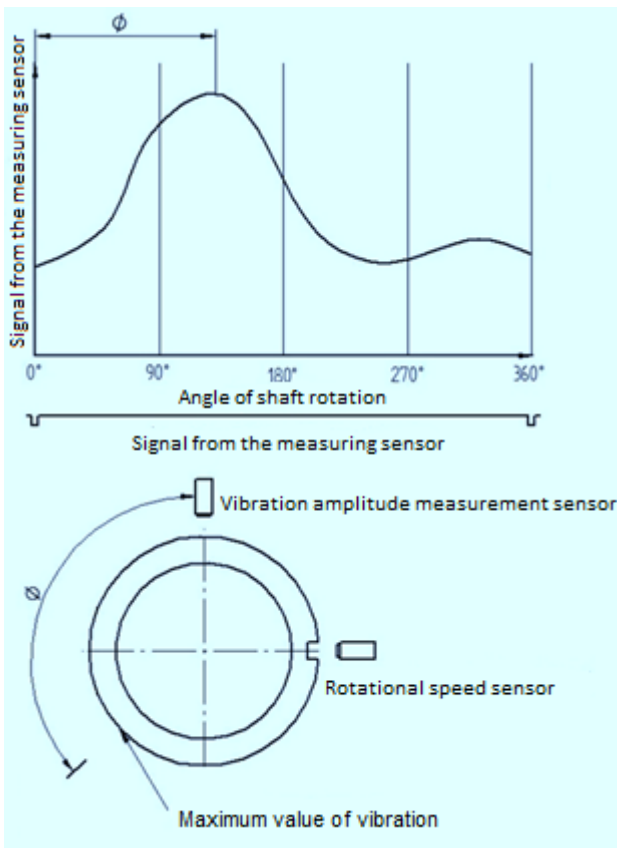


Fig. 7. Presentation of the phase angle of the vibration velocity amplitude (own elaboration)

In order to introduce unbalance, M6 screws and washers of known mass were used, screwed on the perimeter of the disk mounted on the shaft. The phase angle of the unbalance introduced for the test is defined as the angle between the permanently chosen reference plane and the plane passing through the axis of rotation of the shaft and the center of mass of the imbalance introduced (fig. 8).

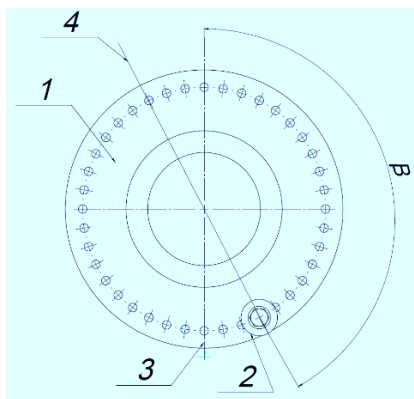


Fig. 8. Illustration of the phase angle of the introduced unbalance β : 1 - a disc used to introduce unbalance, 2 - unbalance, 3 - conventional reference plane, 4 - plane passing through the center of gravity of an unbalance and shaft rotation axis (own work)

Analysis of test results

In the analysis of results, it should be taken into account that the shaft receiving part made low-frequency vibrations in the direction corresponding to the axis of rotation of the shaft. This phenomenon is explained by the fact that at this stage of research it is not possible to eliminate the compensation of the shaft length in the hinge used when using supports in the test stand.

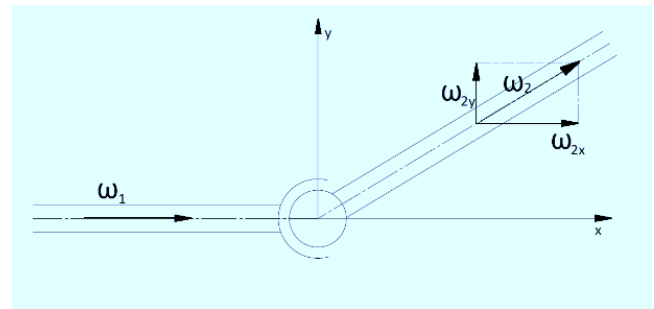


Fig. 9. Illustration of component vector vectors ω_2 (own elaboration)

■ **Reference measurement.** The measurement was made for the zero angle of refraction of the shaft axis and without introducing additional imbalance. The obtained results (fig. 10) indicate the power dependence of the amplitude of the vibration velocity of the shaft from its rotational speed.

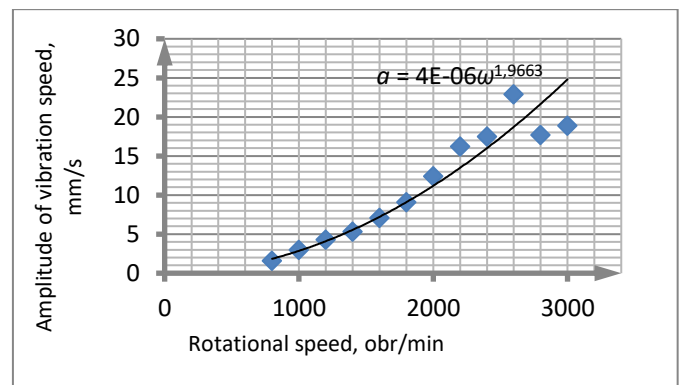


Fig. 10. Results of the reference measurement - the measurement of the vibration velocity amplitude (own elaboration)

The qualitative analysis of the drive shaft system reduced to the linear system - damped viscous and forced inertia - shows that the amplitude of vibration velocity as a function of the rotational speed should change in the square of angular velocity enforcing ω (shaft rotational speed):

$$a = \frac{\frac{m_d * r}{m} * \omega^2}{(\omega_0^2 - \omega^2)^2 + 4h^2\omega^2} \quad (5)$$

where: m_d - unbalance mass, r - unbalance arm, m - reduced shaft mass, $h=c/2m$ (c - damping factor), for subcritical damping:

$$h < \omega_0 = 2\pi f_0 \quad (6)$$

Based on catalog data, natural frequency $f_0 = 2$ Hz.

The trend line in fig. 17 confirms the qualitative change in the amplitude as a function of the rotational speed. The phase angle ϕ of the vibration amplitude should change approximately according to the relationship:

$$\text{tg}\phi = \frac{-2h\omega}{\omega_0^2 - \omega^2} \quad (7)$$

Qualitative analysis (fig. 11) partially confirms this relationship, because the growth dynamics (derivative) is small.

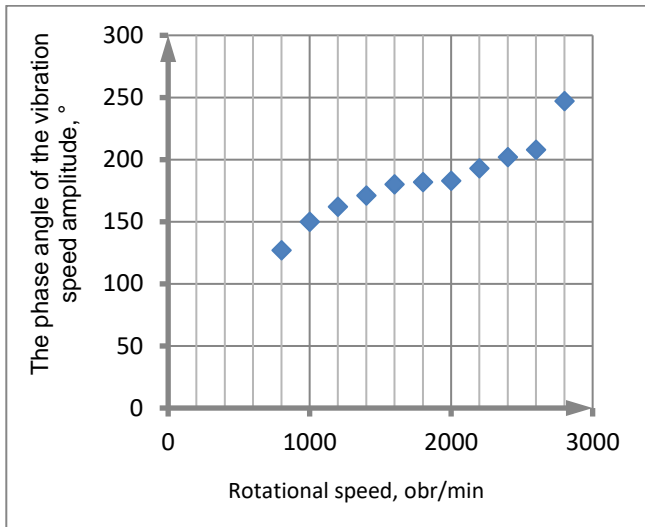


Fig. 11. Results of the measurement of the phase angle of the vibration velocity amplitude in a reference manner (own elaboration)

■ Influence of the angle of the shaft axis on the lateral vibrations of the joint. The studies did not introduce any additional imbalance. Measurements were made for three rotational speeds and for refraction angles from the assumed range. Analysis of the vibration velocity graphs (fig. 12) and its phase angle (fig. 13) indicates that the value of this amplitude is inversely proportional to the angle of refraction of the shaft axis. No relation between the phase angle of the vibration velocity amplitude and the angular angle of the shaft axis deviation outside the range $\gamma = 12.5 \div 15^\circ$ (γ - refractive axis angle) at a rotational speed of 1000 rpm was found. In addition, there was a significant decrease in the phase angle at a speed of 3000 rpm relative to the values measured at 2000 rpm. Determining the causes of this situation requires more thorough analysis.

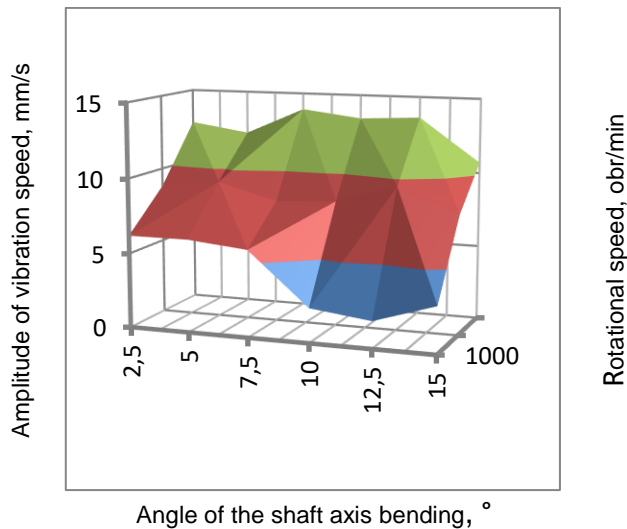


Fig. 12. Collective results of measurements of vibration velocity amplitude depending on the angle of refraction of the shaft axis and rotational speed (own elaboration)

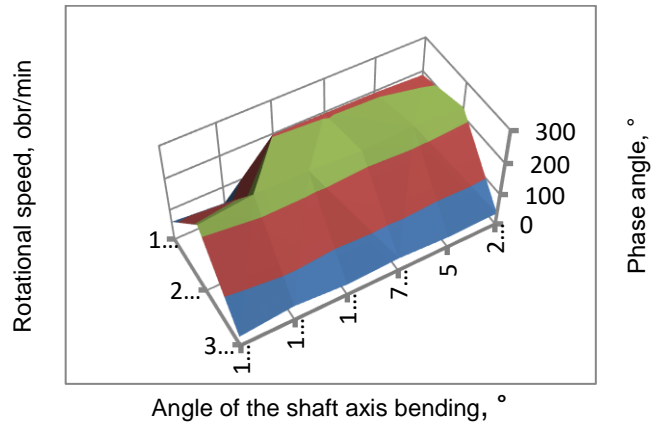


Fig. 13. Collective results of the phase angle measurements of the vibration velocity amplitude depending on the angle of refraction of the shaft axes and the rotational speed (own elaboration)

■ Effect of unbalance introduced in the receiving part of the shaft. The test was carried out at a constant rotational speed of 2,000 rpm. The imbalance introduced ranged from 650 to 2600 g · mm and was always positioned at the same point of the shaft. The graph of the vibration velocity amplitude (fig. 14) shows that its value depends on the imbalance and the angle of fracture of the shaft axis (linearly, inversely proportional).

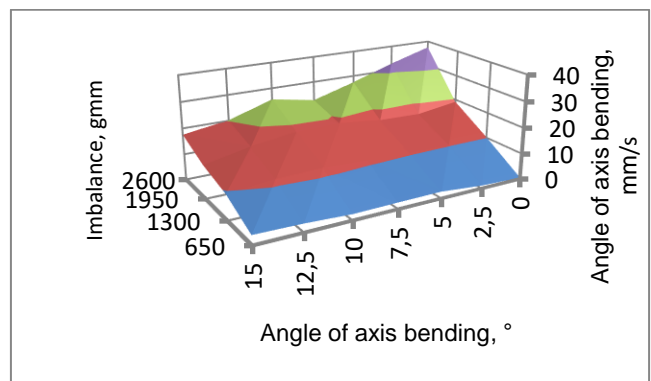


Fig. 14. Dependence of the amplitude of vibration velocity on the angle of refraction of the shaft axis and the imbalance (own work)

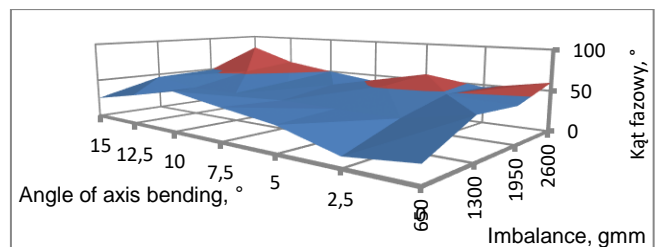


Fig. 15. Dependence of the phase angle of the amplitude of the vibration velocity from non-weighting and the angle of refraction of the shaft axis (own elaboration)

■ Influence of the unbalance phase angle in the driving and driven shaft. In the case described, the value of the unbalance phase angle was changed. For the purpose of further analysis, the course of variation recorded at the shaft speed of 800 rpm (fig. 16) and 2000 rpm (fig. 17) was selected.

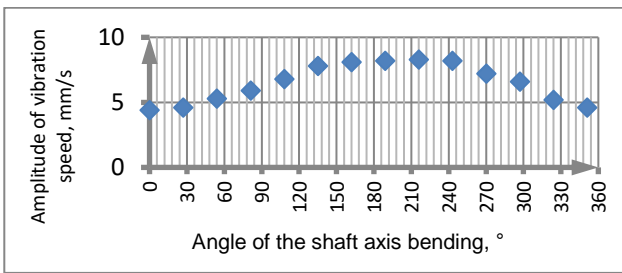


Fig. 16. Course of the variation of the vibration velocity amplitude in relation to the phase unbalance angle at a rotational speed of 800 rpm (own elaboration)

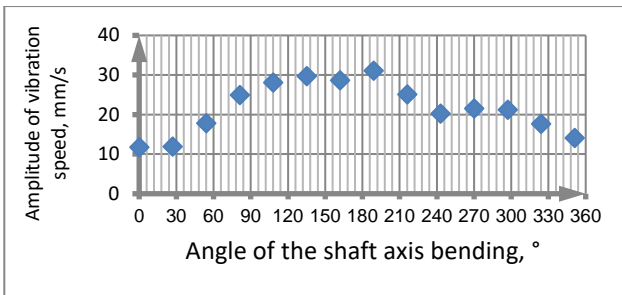


Fig. 17. Course of variation of vibration velocity amplitude in relation to the phase unbalance angle at the rotational speed of 2000 rpm (own work)

Although the second of the analyzed waveforms is clearly distorted by disturbances, the distribution of the measurement points in both cases clearly resembles the course of the sine function. In connection with this, the distribution of measurement points was approximated by performing a functional dependence in the form of:

$$A_v = A \cdot \sin(B \cdot \beta + C) + D \quad (8)$$

where: A_v - vibration velocity amplitude, mm/s; A , B , C , D - function parameters; β - unbalance phase angle, rad.

The values of parameters A , B , C and D were determined using the Microsoft Excel optimization tools (Solver). The parameters were chosen so that the sum of the squares of differences between the measured and calculated values was as small as possible. After the optimization, it was noticed that:

- value of parameter A corresponds to half of the difference between the maximum and minimum value of the amplitude of the vibration velocity in a given series of measurements,
- value of parameter B is approximately 1, so it has no effect on the form of the function.

In addition, the value of parameter C corresponds to the value of 2.5π rad, and the parameter D is equal to the arithmetic mean of all values of the amplitude of the vibration velocity in a given series of measurements.

Using the function parameters determined in this way, the final form of the relationship describing the change in the amplitude of the vibration velocity A_v (in mm/s) was derived depending on the change in the phase angle of the unbalance:

$$A_v = \frac{A_{v_{\max}} - A_{v_{\min}}}{2} \sin\left(\beta + \frac{3}{2}\pi\right) + \bar{A}_v \quad (9)$$

where: $A_{v_{\max}}$ - maximum amplitude in the measurement series, mm/s; $A_{v_{\min}}$ - minimum amplitude in the measurement series, mm/s; \bar{A}_v - average amplitude in the measurement series, mm/s.

In order to verify the correctness of the derivation of the functional dependence, data from the measurement with the

values calculated analytically (fig. 18 and fig. 19) were compiled.

The correctness of the approximation can be confirmed visually only by analyzing the graphs, but additionally it was decided to determine the relative errors of approximation (tab. II).

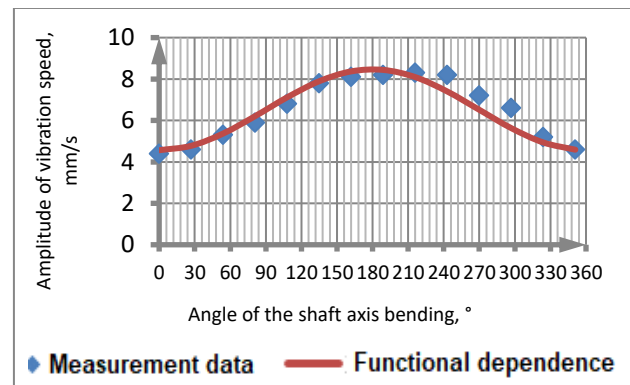


Fig. 18. Comparison of functional dependence with measurement data for $n = 800$ rpm (own study)

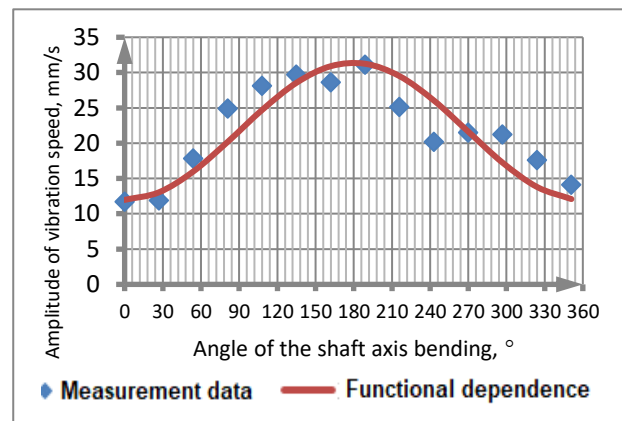


Fig. 19. Comparison of functional dependence with measurement data for $n = 2,000$ rpm (own study)

Large error values in the second measurement result from disturbances occurring when working at high speed. Their source may be the operation of the joint with length compensation or insufficiently rigid mounting of the shaft in the supports. Understanding the exact nature and sources of interference requires additional testing. During the analyzes, the relationship of the phase angle of the vibration velocity amplitude to the unbalance phase angle was also observed. This dependence is linear and is inversely proportional (fig. 20).

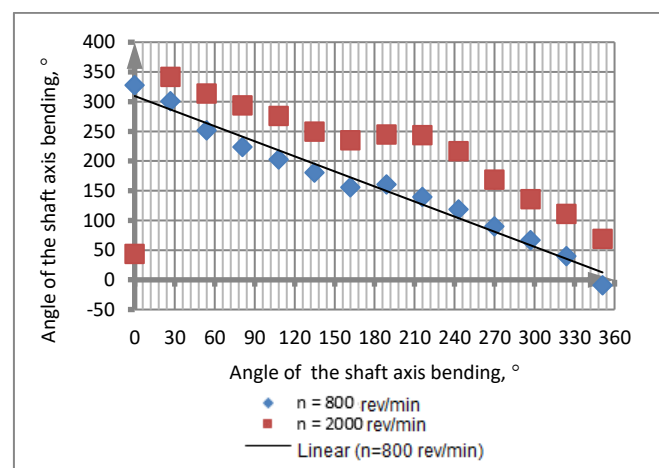


Fig. 20. Dependence of the phase angle of the vibration velocity amplitude on the phase unbalance angle for the tested rotational speeds (own elaboration)

TABLE II. Values of relative errors of function approximation (own elaboration)

$\beta, ^\circ$		0	27	54	81	108	135	162	189	216	243	270	297	324	351
Error, %	n = 800 obr/min	-4	-4	-1	-5	-5	-1	-3	-3	3	10	10	15	5	0
	n = 2000 obr/min	-2	-10	10	19	12	4	-8	0	-18	-29	-1	19	22	14

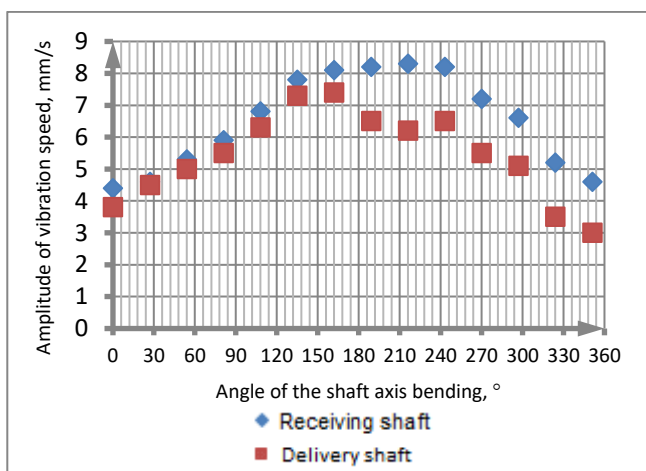


Fig. 21. Comparison of the impact of unbalance introduced in the driven shaft and driving the amplitude of shaft vibration velocity, $n = 800$ rpm (own study)

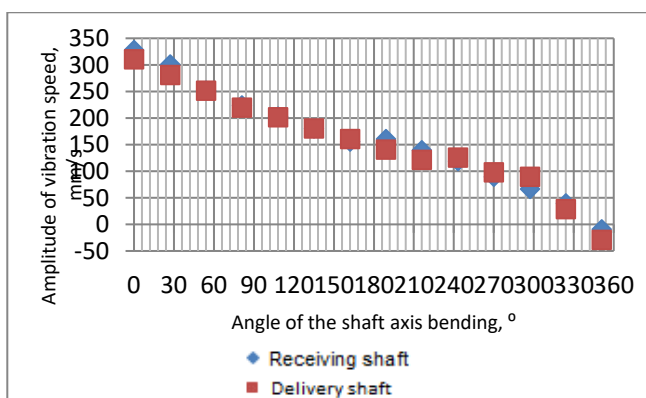


Fig. 22. Dependence of the phase angle of the vibration velocity amplitude from the place of unbalance placement in the tested shaft for $n = 800$ rpm (own elaboration)

The experiment with the unbalance introduced both in the driven shaft and the driving shaft allowed to assess the impact of unbalance placement on the measured values. The values of shaft vibration amplitude for a similar unbalance placed in the driving and driven shaft are shown in one graph (fig. 21). Its analysis allows to conclude that the unbalanced position in the driven (receiving) shaft has a stronger effect on the articulation of the joint.

During the analysis of the impact of unbalance placement on the phase angle value of the vibration velocity amplitude, no correlation between these parameters was found (fig. 22).

Conclusions from the analysis

During the data analysis, several important regularities were noticed:

- increase in rotational speed results in a proportional increase in the amplitude of the vibration speed of the shaft;
- increasing the angle of refraction of the shaft axis causes a decrease in the value of the vibration velocity amplitude, however it has no effect on its phase angle;
- increase in unbalance translates linearly into an increase in the vibration velocity of the shaft and does not affect the value of its phase angle;

- shaft is subject to stronger dynamic phenomena in the event of an imbalance in its driven part;
- placing an unbalance in the driving part has the same effect on the phase angle of the vibration velocity amplitude as placing an unbalance in the part of the driven shaft;
- change in the phase angle of the unbalance translates into a sinusoidal change in the amplitude of the vibration velocity of the shaft, according to the equation (7).

Possibilities for practical application of the results obtained

The development of vibroacoustic models of motor vehicles is a known issue and is already taken up in the literature [14]. In addition, some authors go further in their deliberations and develop diagnostic algorithms based on the analysis of dynamic phenomena occurring in vehicles [5, 12, 13]. The results presented here can be used to develop similar diagnostic models, taking into account the faults of the drive shaft and driveshafts. It is also possible to develop models needed to carry out fatigue and dynamic analyzes with the use of the finite element method (e.g. in the ANSYS program) or mathematical modeling (e.g. in the Matlab program) [7, 8, 17, 18].

The combination of joint wear modeling and diagnostic algorithms can be used to develop a predictive-diagnostic system for the operation of drive train components in vehicles and industrial equipment. The use of such a system would undoubtedly contribute to shortening the downtime and to extending the life of the facilities.

REFERENCES

1. Adams M.L., Jr. "Rotating Machinery Vibration. From Analysis to Troubleshooting". Second edition. Boca Raton: CRC Press, 2010. ISBN 978-1-4398-0717-0.
2. "Bently Nevada TK Velocity Transducer User Guide. Minden: Bently Nevada, 1991.
3. "Bently Nevada TK83 Handheld Balance Master 2 User Guide". Minden: Bently Nevada, 1991.
4. "Bently Nevada TK84 Temporary Transducer Interface User Guide". Bently Nevada. Minden 1992.
5. Dziurdz J. „Diagnozowanie układów napędowych pojazdów oparte na analizie zjawisk nieliniowych". *Przegląd Mechaniczny*. 11 (2014): pp. 26–29.
6. Genuit K. "Vehicle interior noise – combination of sound, vibration and interactivity". *Sound and Vibration*. December 2009: pp. 8–12.
7. Glowinski S., Krzyzyski T., Pecolt S. et al. "Design of motion trajectory of an arm exoskeleton". *Archive of Applied Mechanics*. 85, 1 (2015): pp. 75–87.
8. Hatch M.R. "Vibration Simulation Using Matlab and ANSYS". First edition. Boca Raton: Chapman & Hall/CRC, 2001. ISBN 1-58488-205-0.
9. Heisler H. "Advanced Vehicle Technology". Second edition. Oxford: Butterworth Heinemann, 2002. ISBN 0-7506-5131-8.
10. International Standard ISO 1925. Mechanical vibration – Balancing – Vocabulary. Fourth edition 2001-04-01.
11. International Standard ISO 1940-1. Mechanical vibration – Balance quality requirements for rotors in constant (rigid) state – Part 1: Specification and verification of balance tolerances. Second edition 2003-08-15.
12. Komorska I. "A vibroacoustic diagnostic system as an element of improving road transport safety". *International Journal of Occupational Safety and Ergonomics (JOSE)*. 19, 3 (2013): pp. 371–385.

13. Komorska I. „Detekcja uszkodzeń mechanicznych zespołu napędowego pojazdu na podstawie modelu sygnału drgań”. *Przegląd Mechaniczny*. 11 (2014): pp. 21–25.
14. Kucharski T. „System pomiaru drgań mechanicznych”. Wyd. 1. Warszawa: WNT, 2002. ISBN 83-204-2739-4.
15. Łączkowski R. „Wyważanie elementów wirujących”. Wyd. 1. Warszawa: WNT, 1979. ISBN 83-204-0068-6.
16. Lee H.W., Park S.H., Park M.W., Park N.G. “Vibrational characteristics of automotive transmission”. *International Journal of Automotive Technology*. 10, 4 (2009): pp. 459–467.
17. Maciejewski I.; Glowinski, S.; Krzyżynski, T., Active control of a seat suspension with the system adaptation to varying load mass, *MECHATRONICS*, Volume: 24 Issue: 8 pp: 1242-1253 DEC 2014
18. Maciejewski I., Krzyżynski T., Meyer L. “Control system synthesis of seat suspensions used for protection of working machine operators”. *Vehicle System Dynamics*. 52, 11 (2014): pp. 1355–1371.
19. Micknass W., Popiol R., Sprenger A. „Sprzęgła, skrzynki biegów, wały i półosie napędowe”. Wyd. 2. Warszawa: WKŁ, 2009. ISBN 978-83-206-1575-3.
20. Parszewski Z. „Drgania i dynamika maszyn”. Wyd. 1. Warszawa: WNT, 1982. ISBN 83-204-0341-3. ■

Translation of scientific articles, their computer composition and publishing them on the website www.mechanik.media.pl by original articles in Polish is a task financed from the funds of the Ministry of Science and Higher Education designated for dissemination of science.



Ministry of Science
and Higher Education

Republic of Poland